Very low energy photofission of ^{238}U

C. D. Bowman, I. G. Schröder, and C. E. Dick
National Bureau of Standards, Washington, D. C. 20234

H. E. Jackson
Argonne National Laboratory, Argonne, Illinois 60439

(Received 13 January 1975; revised manuscript received 9 June 1975)

The photofission cross section of ^{238}U was measured in the 2.75- to 5.75-MeV range. Cross sections as small as 2×10^{-11} b were detected. A shelf was observed which had been predicted to occur in the cross section owing to the dominance of radiative decay of levels in the second well. Barrier penetrabilities for both inner and outer barriers were determined from these measurements and together with penetrabilities from other measurements were used to infer a potential shape for ^{238}U. The total γ-ray strength function in the second well at 4.25 MeV was found to be 1.3×10^{-5}. From comparison of expected and measured cross sections at the lowest energies, the density of levels effective in photofission at 3 MeV was found to be greater than 4 per MeV.

[NUCLEAR REACTIONS, FISSION Measured photofission cross section for ^{238}U in the 2.75–6-MeV interval. Deduced details of fission barrier shape and γ-ray decay properties in both inner and outer wells.]

INTRODUCTION

The present strong interest in the study of the fission process and the unique features of the electromagnetic interaction have resulted in several careful studies[1-5] in recent years of the photofission process for ^{238}U. These studies have been directed toward the possibility of "intermediate" structure in the cross section, the study of angular distributions to understand the angular momentum and excitation process involved in photofission, and the derivation of the shape parameters of the inner and outer fission barriers. The measurements were limited to the region above 5 MeV by the rapid fall in the cross section below that energy and thus the parameters derived or phenomena studied related to the region very close to the top of the barrier.

It has been pointed out by Bowman,[6] however, that measurements are possible perhaps to energies lower than 2.5 MeV and that parameters of the fission barrier far below the peaks are manifested in the cross section. The major feature to be expected is a shelf in the cross section in the 3–4.5-MeV region caused by the dominance in the second well of the radiative decay process over the fission process. Photofission on the shelf is predicted to be almost purely isomeric or delayed fission and the slope of the shelf is independent of the parameters of the outer barrier. The intent of the present experiment was to extend the fission measurements to as low an energy as possible so as to verify the existence of the shelf and analyze the results for ^{238}U fission barrier parameters.

EXPERIMENT

The energy range of 2.5–6 MeV is an awkward one for study of photonuclear reactions. Linacs generally are built to operate at higher energy and perform poorly in this energy region. The electrostatic electron accelerator, while capable of an intense and well-controlled beam, usually is not built for energies above 4 MeV. Monoenergetic neutron capture γ-ray beams from a nuclear reactor are not suitable both for reasons of inadequate intensity, fixed energy, and an energy resolution which is very much smaller than the spacing of levels of interest. The Compton scattering monochromator is valuable in terms of resolution and energy variability, but suffers even more with regard to intensity.

It was readily apparent that electron bremsstrahlung would be our most intense source of γ rays for measurements to much lower energies than previously studied. Since the fission cross section is changing so rapidly and in a nearly monotonic fashion over the energy range of interest, the unfolding problem which is so serious in many experiments is of little significance. As the National Bureau of Standards (NBS) possesses a 4-MeV electrostatic electron accelerator and it was clear from the theoretical study that measurements in the 2.5- to 4-MeV region would be necessary for the derivation of useful informa-

tion from the experiment, the first experiments were carried out on that facility.

The experimental apparatus is shown in Fig. 1. The electron beam focused to a 3-mm-diam spot, was incident on a target oriented at 45° to the electron beam. The target consisted of a gold foil of 3-mm thickness backed by a silver foil of 3-mm thickness and supported in a 0.47-cm-thick copper flange arranged to conduct the heat from the beam spot away to a larger surface where it was dissipated by radiation. A depleted ^{238}U foil of 3.2-mm thickness was placed 2.6 mm from the center of the Au target and a mica foil was placed against it so that the γ rays first traversed the mica. Both the mica and the ^{238}U were placed inside of an Al can with a 0.025-cm-thick window. The effective thickness of the ^{238}U in the experiment was determined by the number of fission fragments which escape from an infinitely thick foil. Our calculated value of 4.3 mg/cm^2 has been verified experimentally.[7]

Considerable effort was made to eliminate any known source of background and to verify that no significant backgrounds existed. Calculations indicated that the largest source of background aside from spontaneous fission would come from neutron-induced fission in the 0.4% isotopic contaminant of ^{235}U in the fission foil. At the energies of this experiment the only possible sources of neutrons are the (γ, n) reactions on beryllium and deuterium.

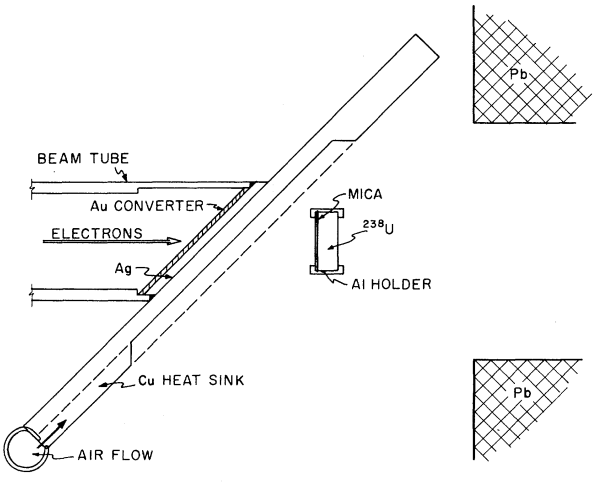

FIG. 1. Apparatus for photofission measurements. The electron beam strikes a bremsstrahlung target attached to a large diameter copper radiator. No water cooling is permitted owing to concern about producing neutrons in the small amount of deuterium present. The lead shield is included to prevent the γ-ray beam from striking a concrete wall 3 m away and creating neutrons from the trace amounts of deuterium and beryllium contained in the concrete.

For this reason water cooling of the target was avoided. Also, an open-faced cubical shell of Pb with 15-cm-thick walls and about 30-cm inside dimension was positioned as shown in Fig. 1. Its purpose was to prevent the bremsstrahlung beam from striking the concrete wall of the room which was about 3 m away and creating neutrons from (γ, n) reactions with the deuterium naturally present in the water of the concrete. Throughout the measurement ^{235}U foils were mounted outside of the Pb shield to monitor the low energy neutron-induced background from ^{235}U fission. The effect was negligible and no corrections were required.

There remained the possibility that there might be Be in the bremsstrahlung target and the foil holder or deuterium in the water vapor in the air in sufficient amounts to create a bothersome background. This source was investigated experimentally by irradiating a ^{235}U foil in place of the ^{238}U foil which is expected to have a much higher sensitivity to neutrons owing to the $1/v$ cross section of ^{235}U. This possible source of background was also found to be negligible.

The measurements were carried out using a 100-μA electron beam which was the limit that the target could withstand without water cooling. The measurements were typically hours in length—the longest measurement being about 40 h for the measurement at an incident electron kinetic energy E_e of 3 MeV. An increase in sensitivity of a factor of 40 would have been available if the target assembly had been redesigned to permit both the use of the 1-mA capability of the accelerator and a repositioning of the ^{238}U closer to the source.

Track detectors were used for this experiment since the fissile sample was located in a very intense γ-ray field which would have made detection of fission events in fission counters exceedingly difficult. Also, the fission rate was very small causing considerable concern that occasional electronic noise pulses might be misinterpreted as fission events. Mica was selected as the track detector since it is the only foil material known to the authors which was capable of withstanding the integrated γ-ray dose.

The existence of geological tracks associated with spontaneous fission of minute amounts of ^{238}U naturally present in the mica was the major liability of the mica detectors. This problem was resolved by means of two procedures. First, the mica was annealed before use in the experiment in an oven for 15 h at 500°C. This annealing removes the large majority of the fission tracks. However, some still remained which apparently could not be removed by annealing. The mica was next etched in HF (48%) for 7 h at room temperature. After irradiation in the experiment the foil

was etched in the same way for 2 h. The geological tracks, therefore, received 9 h of etching whereas the photon-induced fission tracks received only 2 h, thus permitting a clear differentiation between the geological tracks and the photofission tracks by track size or diameter. Since only one side of the mica was in contact with the ^{238}U foil, the difference between the track density on both sides of the foil gives the track density associated with photofission. As a further check on the technique no small diameter tracks were found on the side which was not exposed to the ^{238}U foil.

A correction was required for the spontaneous fission rate of the sample. This was done simply by measuring the time during which the mica was in contact with the sample, and calculating the track-density correction from the known spontaneous fission half-life. For the lowest energy point the spontaneous fission contribution made up half of the observed track density. By improving the solid angle and increasing the beam intensity, significant gains against the spontaneous fission background are possible with existing NBS facilities. However, spontaneous fission can be a serious limitation for other nuclei of interest unless pulsed beam techniques and prompt detection schemes are used to reduce this background.

By the means described above measurements were carried out at electron energies of 3, 3.5, and 4 MeV at NBS. A preliminary study of the results indicated that the cross section appeared to be falling less rapidly with energy than had been seen in other experiments in the 5–6-MeV range pointing toward the existence of the predicted shelf.[6] It was felt that measurements by the same technique were needed in the 4- to 6-MeV range. Since no suitable source was readily available at NBS, the measurements at higher energy were carried out at the Argonne National Laboratory (ANL) electron linear accelerator. The configuration of the experiment was the same as that of the NBS measurements except for the lead cubical shell which was not necessary since the (γ,f) cross section in the 4- to 6-MeV region is higher than at lower energies. Measurements were taken in $\frac{1}{2}$-MeV steps. The results of both experiments expressed in fissions/C cm^2 are given in column 2 of Table I.

The cross section $\sigma(E_\gamma)$ was derived from the yield curve starting with the expression

$$Y_f(E_e) = n\int_0^E \varphi(E_\gamma, E_e)\sigma(E_\gamma)dE_\gamma \ , \qquad (1)$$

where $Y_f(E_e)$ is the fission rate per C cm^2 as a function of electron energy, n is the sample thickness in atoms/cm^2, and $\varphi(E_\gamma, E_e)$ is the spectrum

TABLE I. A summary of experimental results.

Electron energy (MeV)	Fissions/C cm^2	x-ray energy (MeV)	Cross section [a] (b)
3.0	0.11 ± 0.06	2.75	$1.9 \pm 1 \times 10^{-11}$
3.5	5.5 ± 1.6	3.25	$8.2 \pm 2.9 \times 10^{-10}$
4.0	41 ± 4	3.75	$3.5^{c} \pm 0.8 \times 10^{-9}$
4.0	33 ± 6		
4.5	$2.0^{b} \times 10^{2}$	4.25	$3.9 \pm 0.9 \times 10^{-8}$
5.0	$7.5^{b} \times 10^{3}$	4.75	$1.3 \pm 0.3 \times 10^{-6}$
5.5	$2.7^{b} \times 10^{5}$	5.25	$4.4 \pm 1.0 \times 10^{-5}$
6.0	$6.3^{b} \times 10^{6}$	5.75	$1.3 \pm 0.3 \times 10^{-3}$

[a] The uncertainty shown is the quadratic sum of the standard deviation resulting from track counting and an estimated ±20% uncertainty in the bremsstrahlung spectrum. An uncertainty discussed in the text of possibly 50% in the scale factor owing to uncertainty in ΔR is not included.

[b] The standard deviation in tract counting for these points is ±10%.

[c] This point is the average of the points measured at NBS and at ANL.

obtained per C cm^2 for an electron bombarding energy of E_e. This quantity $\varphi(E_\gamma, E_e)$ was determined from the thick-target calculations of Dickinson and Lent[8] which take into account energy loss, multiple scattering, and γ-ray attentuation in the target. An approximation to the solution of Eq. (1) is obtained for $\sigma(E_\gamma)$ by rewriting it in the form of the following set of simultaneous equations

$$Y_f(E_e) = n\sum_{i=1}^{i=E_e/0.5} \varphi(E_{\gamma i}, E_e)\sigma(E_{\gamma i})\Delta E_\gamma \ , \qquad (2)$$

where $\varphi(E_{\gamma i}, E_e)$ has been averaged in $\frac{1}{2}$-MeV intervals and $\sigma(E_{\gamma i})$ is taken as the average value within the $\frac{1}{2}$-MeV interval. The equations were solved by starting first with the lowest energy measurement and working through to the highest energy measurements. Owing to the rapid rise in the cross section there is only a rather small interdependency of one equation on another.

The results with the appropriate γ-ray energies are shown in columns 3 and 4 of Table I. The 4-MeV measurements at ANL and NBS agreed within their uncertainty so that the yields for this point were averaged to obtain one value for the cross section. In addition to the counting statistical uncertainty, an additional uncertainty of ±20% was included owing to the problem of interpolating between the calculations of Dickinson and Lent to obtain the $\varphi(E_{\gamma i}, E_e)$ at $\frac{1}{2}$-MeV intervals. The results are plotted in Fig. 2. For the points above 3.5 MeV the uncertainties are only slightly larger than the size of the points. A normalization un-

certainty of up to ±50% is present owing to solid angle uncertainties common to both the NBS and Argonne measurements. The value of the cross section at 5.75 MeV of 1.3 mb is in satisfactory agreement with the value of about 1.7 mb given by Khan and Knowles[1] who also measure the curvature shown between 5.5 and 6 MeV. The predicted[6] shelf where delayed fission dominates is clearly visible in the cross section curve as is the more rapidly rising region where the prompt fission dominates. The two types of fission appear to be equal at 4.25 MeV. Half the measured cross section at 4.25 MeV is shown by the rectangular point at that energy. This point is used in fitting the measured cross section with two straight lines representing the delayed and prompt components.

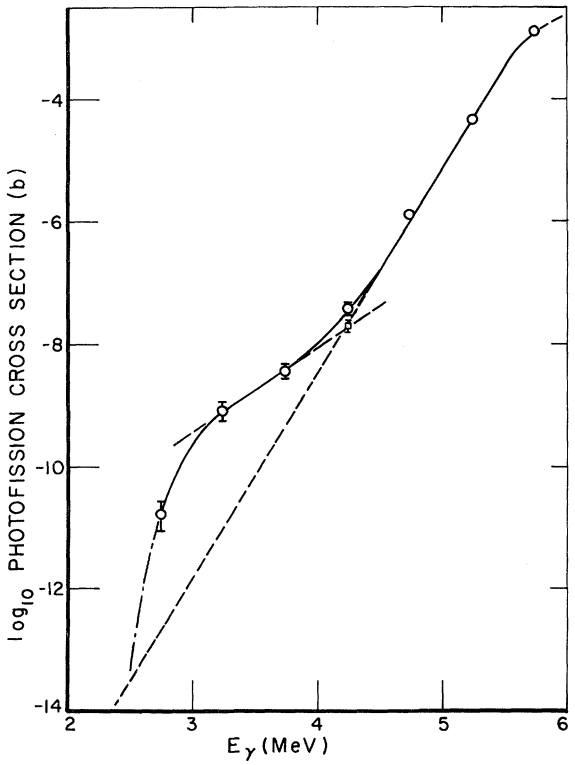

FIG. 2. The photofission cross section of ^{238}U. The two straight dashed lines show the extensions of the regions where either prompt or delayed fission dominates. The dot-dashed curve is included to show the return of the cross section to the dependence on penetration of the full barrier which is predicted to occur below the isomer excitation energy of 2.56 MeV. The uncertainty flags shown do not include systematic uncertainties which are estimated to be of about the same size. When no flags are shown, the uncertainty is only slightly larger than the point size.

ANALYSIS

In Ref. 6 expressions are derived which are intended to describe the photofission cross section in the very low energy region. It is shown there that in the higher energy region (4.5–6 MeV) the prompt fission dominates and that in the lower energy region (< 4 MeV) the delayed fission is largest. After appropriate simplification and evaluation of constants, Eq. (15b) and (15a) are obtained which are reproduced below:

$$\sigma(\gamma, df) = 5.04\times10^{-4} E_\gamma R \exp[2\pi(E_\gamma - E_a)/\hbar\omega_a], \tag{3a}$$

$$\sigma(\gamma, pf) = 5.92\times10^{3} E_\gamma [\exp(-1.6E_\gamma)] \times\{\exp[2\pi(E_\gamma - E_a)\hbar\omega_a + 2\pi(E_\gamma - E_b)/\hbar\omega_b]\}, \tag{3b}$$

where $\hbar\omega_{a,b}$ and $E_{a,b}$ are the curvature and height of the barriers, respectively, and R is the probability for the isomer to decay by fission.

When Eq. (3a) is applied to the shelf, the slope determines a value of $\hbar\omega_a = 2.2 \pm 0.3$ MeV. The uncertainty is obtained by rocking the straight line on the shelf through the point at 3.75 to the limits of the uncertainty flags of the points. For this purpose the point of 4.25 MeV reduced by a factor of 2 has been used since the two types of fission are equal here. The uncertainty obtained in this way is somewhat larger than obtained in a least squares fit, but the more conservative value quoted here is deemed more appropriate. This value is significantly larger than the value of 1 MeV obtained by Back *et al.*[9] via direct reactions and by Alm, Kivikas, and Lindgren[10] from higher energy photofission, both of which were sensitive to the curvature near the top of the barrier. The present value measures the curvature at an energy which is on the average 2 MeV lower than the Back and Alm experiments where the curvature might be expected to be different. The present larger value characterizes a barrier with larger curvature; i.e., one which falls more rapidly than at higher energies.

Russo, Pederson, and Vandenbosch[11] have measured directly the γ-ray decay of the isomer in ^{238}U. From the lifetime for this process assuming a value for $E_a = 6.1$ MeV and a pure parabolic shape, they have derived a value for $\hbar\omega_a$ of 1.2 MeV. These parameters characterize the penetration at the excitation energy of the isomer of 2.56 MeV (also derived in their experiment). Altogether values of $\hbar\omega_a$ now exist at three points on the barrier. If these values were all the same, the characterization of the barriers with the two parabolic parameters of barrier height and curva-

ture would be justified. However, since they are different, it is clear that information is now beginning to become available which would justify a more detailed picture of the barrier shape than is possible with the parabolic parameters.

Instead of attempting to extend the concept of sections of parabolas, we might prefer to deal directly with barrier penetrabilities, if they can be derived from experiment, and use them through the WKB approximation to construct the phenomenological fission barrier. Penetrabilities can indeed be derived from this experiment using Eqs. (3a) and (3b) by substituting the penetrabilities P_a and P_b for the parabolic-based exponential terms so that Eqs. (3a) and (3b) can be rewritten:

$$\sigma(\gamma, df) = 5.04\times10^{-4}E_\gamma R P_a \tag{4a}$$

and

$$\sigma(\gamma, pf) = 5.92\times10^{3}E_\gamma \exp(-1.6E_\gamma)P_a P_b. \tag{4b}$$

Using the measured cross sections of Table I, it is possible to derive the penetrability for both the inner and outer barrier at several different energies. A summary of penetrabilities derived from this experiment and from others is shown in Table II. Using Eq. (4a) above, one can obtain directly the penetrabilities for the inner barrier at 4.25, 3.75, 3.25, and 2.75 MeV. From Eq. (4a) and (4b) together one can obtain P_b at 4.25 MeV. Values for P_a and P_b at 2.56 MeV are a direct result of the experiment of Russo *et al.*[11]

Information at the tops of the barriers can be derived from other experiments which concentrated on the measurement of barrier curvature at the top of the barrier and barrier height. Both Back *et al.*[9] and Alm *et al.*[10] agree on the height and curvature of the inner barrier. These results and the penetrabilities derived from them at 6.0 and 5.5 MeV are given in the table. For the outer barrier the same authors give the same result of 6 MeV for E_b but give somewhat different numbers for $\hbar\omega_b$. Back *et al.* give 0.6 MeV and Alm gives 0.9 MeV. We have chosen a value of 0.7 MeV for $\hbar\omega_b$ weighting the more extensive direct reaction measurements more heavily. The curvature and height of the outer barrier have been used to calculate P_b at 6.0 and 5.25 MeV.

Two more significant penetrabilities can be derived from these experiments. Since the value of P_b at 5.25 MeV is obtained from other experiments and a value for $P_a P_b$ can be obtained at that energy using Eq. (4b), a value for P_a at 5.25 MeV of 9×10^{-3} can be derived.

A value for P_b at 4.75 MeV is obtained again using a value of $P_a P_b$ derived from Eq. (4b) and a value of P_a derived in the following way. Briefly stated the many values of P_a available above and below 4.75 MeV determine the value for P_a at 4.75 MeV to be 2×10^{-3}. This is shown in parenthesis in Table II since it was inferred rather than obtained directly from experiment. This value then implies a value for $P_b = 4\times10^{-5}$ at 4.75 MeV from the measured cross section and Eq. (4b).

A barrier can now be constructed using this table of penetrabilities. The basis for this is the use of the WKB approximation employed in the Hill-Wheeler[12] study of fission barrier penetrability

$$P = 1/(1+\exp\gamma) \simeq \exp(-\gamma), \tag{5a}$$

where

$$\gamma = \text{const}\int [V(\delta) - E]^{1/2} d\delta \tag{5b}$$

and the integral is taken over all area between E and the curve $V(\delta)$. For the purposes of this paper δ has been chosen such that when V is expressed in MeV, the constant in Eq. (5b) is unity.

We begin the barrier construction on barrier a with a parabolic shape with curvature of 1 MeV and height 6 MeV extending down to 5.5 MeV as shown in Fig. 3 at $\delta = 15$. The next value for P_a

TABLE II. Experimentally determined barrier penetration parameters.

Energy	P_a	Source	P_b	Source
6.0	0.5	E_a=6 MeV, $\hbar\omega_a$=1 MeV	0.5	E_b=6 MeV, $\hbar\omega_b$=0.7 MeV
5.5	4×10^{-2}			
5.25	9×10^{-3}	from $P_a P_b$	7×10^{-4}	
4.75	(2×10^{-3})		4×10^{-5}	from $P_a P_b$
4.25	4×10^{-4}	P_a	2×10^{-6}	P_b
3.75	9×10^{-5}	P_a		
3.25	2×10^{-5}	P_a		
2.75	6×10^{-7}	P_a		
2.56	2×10^{-8}	Russo *et al.* (Ref. 11)	5×10^{-16}	Russo *et al.* (Ref. 11)

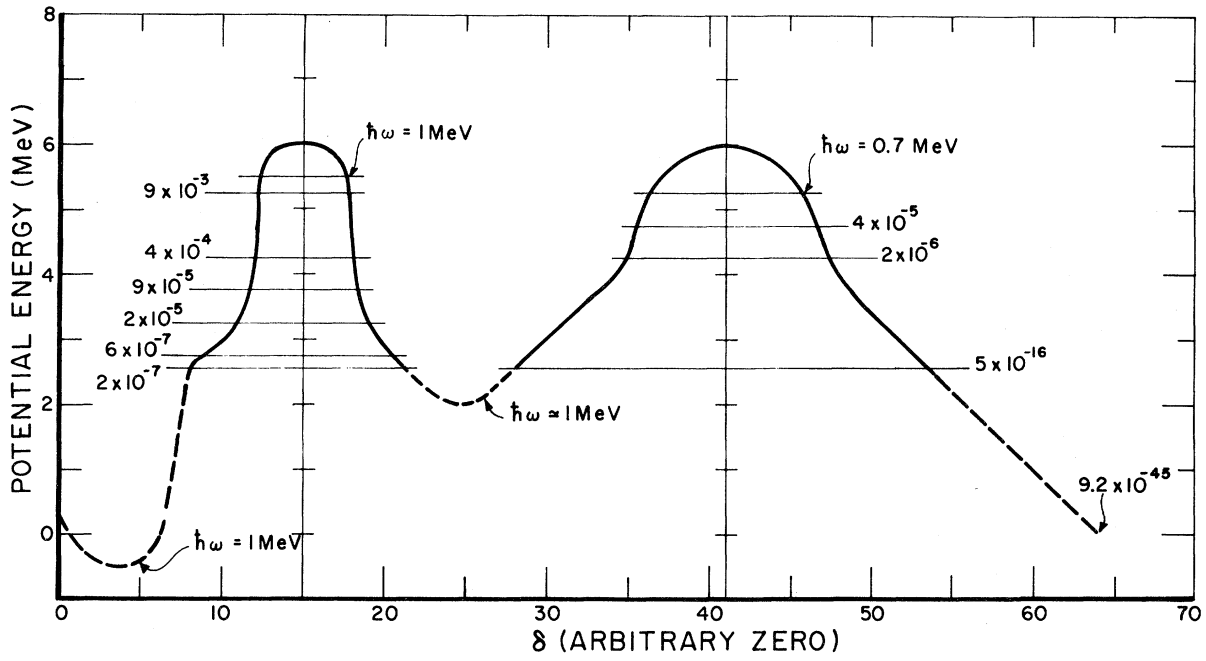

FIG. 3. The potential barrier for ^{238}U. The curve is constructed from barrier penetrabilities derived from this and other experiments. These penetrabilities are given in the figure. The scale for the deformation parameter δ is chosen to simplify calculations as described in the text. The zero for δ has been chosen arbitrarily. The value shown at the far right of the figure of 9.2×10^{-45} is the penetrability corresponding to ground state spontaneous fission.

$=9\times10^{-3}$ is found at 5.25 MeV. By trial and error Eq. (5b) is numerically integrated until the proper shape is found to yield the correct value for P_a at that energy. Using the curve determined for higher energies this process is repeated until the lowest value at 2.56 MeV has been included. The resulting curve, smoothed somewhat, is shown in Fig. 3 by the solid line. The value of Russo *et al.* at 2.56 MeV of $P_a=2\times10^{-8}$ requires a marked flattening of the curve. Since this penetrability depends on a rough estimate of the γ-ray transition probability in well a, the actual penetrability used in Fig. 3 was increased by a factor of 10 to obtain consistency with the other data without significantly distorting the interpretation of the Russo experiment. Barrier b constructed in the same way is also shown as a solid line. Assuming a parabolic curvature for the minimum between barriers of $\hbar\omega=1$ MeV following Russo[11] and the harmonic oscillator relationship $E=E_0+(n+\frac{1}{2})\hbar\omega$ results in a parabola with a minimum at 2.06 MeV which was used to connect the inner and outer barriers. It is shown as a dashed line.

The final piece of available information on the fission barrier which has not yet been used is the spontaneous fission half-life of ^{238}U. The most recent measurement[13] of this half-life yielded the value $t_{1/2}=(1.01\pm0.03)\times10^{16}$ yr. The spontaneous fission mean life can be obtained from the product of the barrier penetrability $\rho=e^{-\gamma}$ and the rate r at which the barrier is attacked which is given by $r=\omega/2\pi$. From Coulomb excitation measurements,[14] a $K=0$ B-vibrational bandhead in ^{238}U has been observed at 0.993 MeV. Through the formula for the levels of a harmonic oscillator, the value for $\hbar\omega$ is found to be $\simeq1$ MeV, which corresponds to a rate of 2.5×10^{20}/sec. A penetrability of 9.2×10^{-45} is obtained from the expression $t_{1/2}=(\ln2)/rP$. The shape of the curve beyond $\delta>54$ and $\delta<8$ can then be adjusted to give the ground state penetrability. For $\delta>54$, the slope at $\delta=54$ has been extended down to zero energy. If the same procedure is followed on the inner curve, the resulting penetrability is much too large. A parabola with curvature of 1 MeV was therefore included as the dashed line attached at $\delta=8$. Penetration of the full barrier then yields the measured ground state penetrability.

The degree to which the barrier of Fig. 3 approximates the real barrier for ^{238}U is unclear. In the first place both the inner and outer barriers have been assumed to be symmetric which is probably not the case. The most obvious adjustment from Fig. 3 might be a skewing of the barrier inward at the base to avoid the rapid change of slope near $\delta=8$. Second, while the procedure for going

from cross section to penetrability seems sound to the authors, we see no easy way to confirm this except through careful measurements of the elastic and total scattering of γ rays below 6 MeV—a measurement which up to now has not been done with the necessary degree of thoroughness. There is also the matter of constancy of the mass constant through the fission process. Nevertheless, we believe that these low energy photofission experiments make it practical to begin attempting to infer the details of the barrier shape. The interpretation of measurements such as this on all six of the available uranium isotopes would be especially interesting in this regard.

COMMENTS AND OTHER RESULTS

For a curvature of $\hbar\omega = 1$ MeV at the bottom of the first well, the $n = 1$ vibrational state should exist at an excitation energy of about 3.65 MeV and the penetrability of the full barrier is expected to be greatly enhanced immediately in the neighborhood of this resonance.[15] It might, therefore, be expected that the cross section should show a strong peak at that energy; or, in terms of the bremsstrahlung yield curve, the curve should show a change of slope at that energy. Such a state is not observed in this experiment. If such a state played a dominant role, the yield would increase only in proportion to the γ-ray intensity being sampled as the electron energy is changed. The change in yield observed is far greater than this effect could explain. Therefore as the energy increases, a number of states with, on the average, ever higher barrier penetrability contribute to the cross section.

Our lowest energy measurement is carried out at an electron energy of 3.0 MeV. The cross section measured is therefore the sum of the contributions from all of the levels in the 2.56- to 3-MeV energy range. The measured cross section, therefore, should be greater than that through the ground state. Using Russo's parameters this photofission cross section can be calculated. By comparison of the measured and calculated values, one can obtain crude information on the number of states in this region contributing to the cross section.

The photofission cross section through a single state can be given in the Breit-Wigner form as

$$\sigma(\gamma,f) = \frac{4\pi\lambda_\gamma g_\gamma \Gamma_{\gamma 0}\Gamma_f}{(E-E_0)^2 + \frac{1}{4}\Gamma^2}. \tag{6}$$

Russo[11] gives lifetimes for γ-ray decay to the ground state, for decay by fission, and for all γ-ray decay processes. These lifetimes can be converted through the uncertainty principle to values for $\Gamma_{\gamma 0}$, Γ_f, and $\Gamma\gamma$, respectively. The value for $\Gamma_{\gamma 0}$ is actually not the same in γ decay and photofission. The decay takes place from the 0^+ isomeric state to the 2^+ rotational state built on the ground state. In photofission the transition is from the 0^+ ground state to the 2^+ rotational state built on the 0^+ isomeric state. This 2^+ state then decays to the 0^+ isomeric state from which fission takes place. In the calculations which follow, we assume that these values for $\Gamma_{\gamma 0}$ are equal since in both cases the change in deformation is the same, the change in spin is the same, and the initial and final state spins are the same. Carrying through the integral and calculating the fission rate for 3-MeV electrons, one obtains an expected rate of 0.025 ± 0.015 fissions/cm^2 C. The errors are based on the uncertainties in Russo's values for the lifetimes of the various decay modes of the isomeric state.

This value is a factor of 4 smaller than the measured rate of 0.11 ± 0.03 fissions/cm^2 C, thus implying the existence of fission through a few more states than the 2^+ rotational state. This analysis would infer a density of states accessible through the electromagnetic process (probably limited to 1^- and 2^+ states) at 2.75 MeV of greater than 4 per MeV.

As pointed out in the companion paper,[6] the ratio of the prompt and isomeric fission cross section can be used to measure the total γ-ray strength function in the second well $\Gamma_{\gamma b\mathrm{II}}/D_{\mathrm{II}}$. At the energy where prompt and delayed fission are equal, which occurs at the onset of the shelf, this quantity is given by

$$2\pi\frac{\Gamma_{\gamma b\mathrm{II}}}{D_{\mathrm{II}}} = \frac{1}{R}\exp(-\gamma). \tag{7}$$

The strength function is found to be $\Gamma_{\gamma b\mathrm{II}}/D_{\mathrm{II}} = 1.3 \times 10^{-5}$ which is significantly smaller than the "measured" value[6] for the first well of $\Gamma_{\gamma a\mathrm{I}}/D_{\mathrm{I}} = 3.7 \times 10^{-4}$ at the same energy.

Lynn[16] has estimated $\Gamma_{\gamma b\mathrm{II}}$ to be a few times smaller than $\Gamma_{\gamma a\mathrm{I}}$. A value can be obtained from the above strength functions using the value of $D_{\mathrm{II}}/D_{\mathrm{I}} = 30$ from Ref. 6 in the expression

$$\frac{\Gamma_{\gamma b\mathrm{II}}}{\Gamma_{\gamma a\mathrm{I}}} = \frac{\Gamma_{\gamma b\mathrm{II}}}{D_{\mathrm{II}}}\left(\frac{\Gamma_{\gamma a\mathrm{I}}}{D_{\mathrm{I}}}\right)^{-1}\frac{D_{\mathrm{II}}}{D_{\mathrm{I}}}. \tag{8}$$

The result is $\Gamma_{\gamma b\mathrm{II}}/\Gamma_{\gamma a\mathrm{I}} = 1.0 \pm 0.7$ at 4.25 MeV where the error is estimated from compounding the uncertainties in the input parameters.

CONCLUSION

Photofission measurements extending down to $E_\gamma = 2.75$ MeV have demonstrated the existence of a predicted shelf[6] in the cross section. The results have been analyzed to obtain barrier pa-

rameters which, when combined with information from other experiments, begin to offer the possibility of a detailed picture of the fission barrier for ^{238}U.

Photofission measurements on a number of nuclei at very low energies would be especially helpful since the systematics for shape characterization of the fission barrier and for the barrier-dependent parameters measured in the present experiment can be determined. The principal limitation in such measurements is the spontaneous fission half-life which can be a serious problem for several targets of interest when the present experimental technique is used.

---

[1]A. M. Khan and J. W. Knowles, Nucl. Phys. A179, 33 (1972).

[2]O. Y. Mafra, S. Kuniyoshi, and J. Goldemberg, Nucl. Phys. A186, 110 (1972).

[3]N. S. Rabotnov, G. N. Smirenkin, A. S. Soldatov, L. N. Usachev, S. P. Kapitza, and Yu. M. Tsipenyuk, Yad. Fiz. 11, 508 (1970) [Sov. J. Nucl. Phys. 11, 285 (1970)].

[4]A. Alm, T. Kivikas, and L. J. Lindgren, in *Proceedings of the International Conference on Photonuclear Reactions and Applications, Asilomar, 1973*, edited by B. L. Berman (Lawrence Livermore Laboratory, Univ. of California, 1973), paper No. 5D6, p. 645.

[5]A. Manfredini, L. Fiore, C. Ramorino, H. G. DeCarvalho, and W. Wolfli, Nucl. Phys. A123, 664 (1969).

[6]C. D. Bowman, preceding paper, Phys. Rev. C 12, xxx (1975); in *Proceedings of the International Conference on Photonuclear Reactions and Applications, Asilomar, 1973* (see Ref. 4), paper No. 5D135, p. 659.

[7]R. Gold and R. J. Armani, Nucl. Sci. Eng. 34, 13 (1968).

[8]W. C. Dickinson, and E. M. Lent, Lawrence Livermore Laboratory, Livermore, California, 1968 Report No. UCRL-50442 (unpublished).

[9]B. B. Back, O. Hansen, H. C. Britt, and J. D. Garrett, Phys. Rev. C 9, 1924 (1974).

[10]A. Alm, T. Kivikas, and L. J. Kindgren, in *Proceedings of the Third International Symposium on the Physics and Chemistry of Fission, Rochester, 1973* (IAEA, Vienna, Austria, 1974), paper No. IAEA/SM-174/36.

[11]P. A. Russo, J. Pederson, and R. Vandenbosch, in *Proceedings of the Third International Symposium on the Physics and Chemistry of Fission, Rochester, 1973* (see Ref. 10), paper No. IAEA/SM-174/96.

[12]D. L. Hill and J. A. Wheeler, Phys. Rev. 89, 1102 (1953).

[13]R. L. Fleischer and P. B. Price, Phys. Rev. 133, B63 (1964).

[14]Y. A. Ellis, Nucl. Data B4, 635 (1970).

[15]J. D. Cramer and J. R. Nix, Phys. Rev. C 2, 1048 (1970).

[16]J. E. Lynn, in *Proceedings of the Second International Atomic Energy Agency Symposium on Physics and Chemistry of Fission, Vienna, Austria, 1969* (IAEA, Vienna, Austria, 1969), paper No. SM-122/204, p. 249.